Stepwise synthesis of cellulose-based polyelectrolyte for generation of Ag-AgCl NPs for medical antibiofilm applications

Amir Hasanzadeh
Maragheh University of Medical Sciences
Salman Shojaei
Iran University of Science and Technology
Behnam Gholipour
Iran University of Science and Technology
Parviz Vahedi
Maragheh University of Medical Sciences
Sadegh Rostamnia (srostamnia@gmail.com)
Iran University of Science and Technology https://orcid.org/0000-0001-6310-8754

Research Article

Keywords: Macromolecules, Cellulose, Polyelectrolyte, Ionic Liquid, Ag-AgCl NPs, Antimicrobial effect

Posted Date: April 20th, 2022

DOI: https://doi.org/10.21203/rs.3.rs-1340431/v1

Abstract

In biomedical applications, biocompatible and nontoxic compounds are the most important types of cytotoxic effects. In this work, the polyelectrolyte Cell/IL/Ag-AgCl NPs were fabricated by immobilizing of Ag-AgCl nanoparticles on the surface of organic biopolymer (cellulose) without using any reducing agent. The physical and chemical properties of polyelectrolyte were characterized by various techniques including TEM, SEM, EDX, XRD, FT-IR, and AAS. The in-vitro antibacterial activity of Cell/IL/Ag-AgCl NPs was investigated on methicillin-resistant *staphylococcus aureus* (ATCC-43300) and multidrug-resistant *Pseudomonas aeruginosa* (ATCC-27853). The results illustrated that the antimicrobial effect of Cell/IL/Ag-AgCl NPs against *Pseudomonas aeruginosa* was higher than that of *Staphylococcus aureus* and also by using the microtiter plate method, the antibiofilm effect of this compound against *Pseudomonas aeruginosa* was remarkable. It is expected that the use of these biocompatible compounds can inhibit the biofilm formation of bacteria on surfaces and equipment, to reduce nosocomial infections, in hospital environments, especially in the intensive care unit, surgery unit/room.

Introduction

With the gentle progress of the population's environmental awareness and living standards, research for the development of biomaterials is increasing(Devi and Ahmaruzzaman 2016; Wu et al. 2017; Carvalho et al. 2019; Leonel et al. 2019; Heidarpour et al. 2020). For this purpose, many efforts pertinent to antibacterial medications and also antibiotic resistance of bacteria have been investigated and inorganic nanoparticles(Vargas-Reus et al. 2012) including Au(Kalwar and Shen 2019a), Ti(Azis et al. 2021; Ebrahimi et al. 2021), Cu(Ruparelia et al. 2008), MgO(Jin and He 2011), ZnO(Pasquet et al. 2014), and Ag(Rostamnia et al. 2016; Lv et al. 2019; Hasanzadeh et al. 2021; Sattari et al. 2021; Dong et al. 2021) have been used to reduce the risk of public health. In this regard, silver and its derivatives (AgCl NPs and Ag-AgCl NPs) due to having thermal stability, good pollution resistance, potent anti-bactericidal ability, health, and environmentally have been attracted to use in widespread applications including catalysis(Han et al. 2014), optics(Wang et al. 2011), nanoelectronics(Van Den Hurk et al. 2013), treatment of various diseases and medical biomedicine(León-Silva et al. 2016). In spits of high immense applications, several successful methods have been developed for the preparation of silver halides. For example, A green method has been reported using Sasa Borealis extract to synthesize Ag-AgCl-NPs and assessed their anticancer properties versus the ventral adenocarcinoma cells(Patil et al. 2017). Khayati and coworkers conveyed that Ag-AgCl-NPs indicated meaningful anticancer activity against MDA-MB-468 cell lines(Sattari et al. 2021). However, the colloidal form of Ag and AgCl nanoparticles have some hitches, for instance easily aggregation, negligible dispersion, fast release, and poor storage constancy which restrict their feasible application and their antibacterial activity(Hasanzadeh et al. 2021). To solve these problems and/or enhance the antibacterial activities, various organic/inorganic support such as natural polymers(Wang et al. 2020), silica(Rostamnia et al. 2016), carbon materials(Vilamová et al. 2019), MOF(Hayati et al. 2021), titanium dioxide(Guan et al. 2019) has been used to stabilize silver nanoparticles. Among these materials, the usage of renewable supports including polysaccharides is

valuable due to being readily available, inexpensive, environmentally friendly, renewable in nature, and high specific surface area(Yuan et al. 2021).

Cellulose nanocrystals (CNCs) are well-known and the most abundant natural biopolymer in the world due to their favorable features for example non-toxicity, biodegradability, and large specific surface area are widely used in medicine and biotechnological, personal care products, nanotechnology fields(Moon et al. 2011; Mohammed et al. 2018). Cellulose can be used as efficient bifunctional fillers and nanofibres for antibacterial activities by incorporating antibiotic materials such as ofloxacin(Qi et al. 2015), Ag NPs, or other metallic and metal oxide NPs(Smiechowicz et al. 2018). Cellulose based on its porous structure and plentiful active sites is an attractive candidate to employ as modified support for immobilizing the metal nanoparticles(Klemm et al. 2011). To succeed in the maximum loading capacity of metals on biopolymer, the surface of CNCs can be improved with desired functional groups(Ghasemi et al. 2016; Rahimi et al. 2017). Furthermore, groups containing positively and negatively charged functional groups including imidazolium(Shojaei et al. 2017a), hydroxyl (-OH), and carboxyl (-COOH) groups(Ko et al. 2015) not only raise the number of active sites and improve the scattering of nanoparticles and superior resistance to agglomeration but also can be reduced metal ions (Ag+) to zero-valent or different form(Vilamová et al. 2019). One of the attractive candidates for these purposes is imidazolium salts that supreme thermal stability and ionic conduction as unique characteristics have enthused the modification of supports with ionic liquids(Shafiei-Irannejad et al. 2019; Qin et al. 2022). Imidazolium salts embedded polymeric supports due to having superb surface charge density, can proliferation the coordination of the metallic ions and mend their diffusing and stability on the polymeric surface(Pinkert et al. 2009). Thus, to develop a simplistic synthetic route with nontoxic and stable support to immobilize Ag nanoparticles on a polymeric skeleton with a high surface area are fascinating and significant.

In continuance of our endeavor in the extension of new systems for medical applications herein, we aimed to develop a facile synthesis of Ag-AgCl NPs and increase the efficiency of silver (Ag-AgCl NPs) as an antibacterial agent by designing a multi-branch biopolymer with ionic groups. The modified cellulose could ameliorate the stability of silver nanoparticles owing to the existence of branched polyionic polymers. Apart from silver (Ag-AgCl), imidazolium moiety seems to be an effective site as another antibacterial agent(Riduan et al. 2016). This route is a powerful approach for the synthesis of Ag-AgCl nanoparticles that avoids the usage of any external halide ion sources, reducing and capping agents which in $AgNO_3$ react with a chloride ion grafted imidazolium salts. The antibacterial activity of synthesized polyelectrolyte (Cell/IL/Ag-AgCl NPs) was investigated on methicillin-resistant *staphylococcus aureus*(ATCC-43300) and multidrug-resistant *Pseudomonas aeruginosa*(ATCC-27853). In-vitro cytotoxicity tests via MMT assay exhibited good biocompatibility for designed polyelectrolyte and could be an apposite candidate for medical uses.

Experimental

Materials and methods

All solvents and materials were purchased from Aldrich, Merck, and Fluka Company. FT-IR spectra were achieved with a Bruker Tensor 27 spectrometer. Elemental analyses were approved with Vario EL (III) system. XRD evaluations were executed by using a Siemens D500 diffractometer (Cu Kα radiation). TEM images were obtained on a JEOL JEM-2000EX with a voltage of 80-200 kV. SEM and EDX analyses were provided with a FEG-SEM MIRA3 (TESCAN) at 30 kV. Ag amount was obtained through flame atomic absorption spectrometer (FAAS) using an air–acetylene flame (model Shimadzu AA-680).

Synthesis of 1-methyl-3-oxiran-2-ylmethyl-1*H*–imidazole-3-ium chloride

To a flask equipped (100 ml) with a reflux condenser, 50 mmol of 2-Chloromethyl oxirane and 50 mmol of 1-methylimidazole were transferred and stirred at 70 °C for 24 h under nitrogen atmosphere. After washing with ethyl acetate to eliminate unreacted raw materials, the product was finally afforded as a brown liquid(Shojaei et al. 2017b).

Preparation of ionic liquid anchored cellulose (Cell/IL)

To a 20 ml of DMF in Schlenk flask, 1.0 g of microcrystalline cellulose and 3.0 g of sodium methoxide were added. The mixture reacted under inert ambient for 1 h at 60 °C and was evacuated under vacuity to remove solvents to obtain the cellulose alkoxide. Then, 1-methyl-3-oxirane-2-yl-methyl-1*H*-imidazolium chloride and cellulose alkoxide were added into 20 ml of dry DMF in the Schlenk flask, and the mixture was stirred at 60 °C for 24 h. Finally, the product was washed with solvents and was dried under vacuum(Shojaei et al. 2017b) and Elemental analysis was carried out for Cell/IL: C (46.05%), H (6.71%), and N (7.12%).

Detection of chloride ion by Mohr's method

Cell/IL (4.0 g) was added in deionized water (50 ml) and then chloride ions of the polymer were determined by precipitation titration with silver nitrate. When $AgNO_3$ solution is dropwise added to the mixture, silver chloride was precipitated. To determine the endpoint of the titration, potassium chromate was placed in the mixture as an indicator. Residual silver ions react with the indicator to obtain red-brown precipitation of the silver chromate. The number of chloride ions in the Cell/IL was determined to be 0.954 mmol g^{-1} (Shojaei et al. 2017b).

Preparation of Cell/IL/Ag-AgCl NPs

In a typical route, to a mixture of 1.0 g of Cell/IL in 50 ml of deionized water, 0.5 g of $AgNO_3$ was added. After reacting at 30 °C for 24 h, the precipitate was isolated and then dried under vacuum at 60 °C for 5 h to obtain Cell/IL/Ag-AgCl NPs.

Measurement of Ag loaded on Cell/IL/Ag-AgCl NPs

To a solution of HCl-HNO_3 (1:3), (10 ml), Polyelectrolyte (Cell/IL/Ag-AgCl NPs) (0.05 g) was added and stirred for 3 h. The residue was filtered and by adding distilled water, the total volume of the solution was

increased to 30 ml and the blank solution containing Cell/IL was also prepared. Finally, by using FAAS analysis, the amount of Ag ions in the polyelectrolyte was determined to be 6.39.

Antibacterial activity assay

Antibacterial activity of the synthesized nanocomposite Cell/IL/Ag-AgCl NPs was assessed against gram-negative *Pseudomonas aeruginosa* (ATCC-27853) and Gram-positive *Staphylococcus aureus* (ATCC-43300) bacteria. In the present study, at first, Minimum Inhibitory Concentration (MICs) of Cell/IL/Ag-AgCl NPs against bacteria by the broth microdilution method was determined. Then, according to the MIC results, Minimum Bacteriocidal Concentration (MBCS) was tested. Clinical and Laboratory Standards Institute guidelines (CLSI) were used for these methods. Eventually, the antibiofilm effect of the Cell/IL/Ag-AgCl NPs was approved by the microtiter plate method for deterrence of bacterial adherence to an abiotic area. All of the inseminated media were incubated at 37 °C for a prolonged time (16-18 h) and the results were certified after three times repeated experiments.

Cell viability test

Human intestinal Caco-2 cells with an antibiotic antimycotic solution (1% v/v) and fetal bovine serum (20% v/v) were cultured in Eagle's minimum essential medium. Caco-2 cells were cultured by using 150 µL of the fresh medium in 96-well microplates (density of 10^5 cells/mL) and then were incubated under modulus conditions (37 °C, 5% CO_2, and 95% humidity). Next, cells were handled with different concentrations (0, 100, 200, 300, 400 ppm) of Cell/IL/Ag-AgCl NPs at 37 °C for 24-hour. Then, rinsed with phosphate-buffered saline and MTT assay (3-(4,5-dimethylthiazol)-2-diphenyltetrazolium bromide) was conducted using 10 µl of MTT reagent per each well, and cells were incubated to determine the cell viability(Nguyen et al. 2017).

Results And Discussion

Characterization of the Cell/IL/Ag-AgCl NPs

The synthesis of polyelectrolyte cellulose-based macromolecule was expertly designed using the following steps as presented in Scheme 1.

The synthesis process of Ag-AgCl NPs immobilized on Cell/IL was described as follows (a) At first, to a mixture of microcrystalline cellulose in dimethyl formamide (as a solvent), 1-Methyl-3-(oxirane-2-yl-methyl)-1*H*-imidazolium chloride was placed to give the ionic liquid anchored cellulose (Cell/IL). (b) Continuing, $AgNO_3$ was added to an aqueous solution of Cell/IL and then the reaction was pursued 24 h at 30 °C to create the Cell/IL/Ag-AgCl NPs polyelectrolyte (Fig. 1). Flame atomic absorption spectrometry (FAAS) was applied to specify the percentages of Ag ions loaded on the polyelectrolyte to be 6.39 wt%.

The synthesized materials were characterized using FT-IR spectroscopy. As presented in Fig. 2(a), in the cellulose spectrum, the wide peak at 3344 cm^{-1} is affiliated to the stretching vibrations of the hydroxyl

group in the biopolymer. The peak at 2895 cm^{-1} relates to stretching vibrations of the CH_2 groups and the absorption peak at 1596 cm^{-1} is associated with the bending mode of the physically absorbed water. The peaks at 1434, 1378, and 1328 cm^{-1} are assigned to the bending vibrations of the C–H bond. The bonds at 1167, 1116, and 1058 cm^{-1} are ascribed to asymmetric bridges stretching the C–O bond, the crystal absorption bond at cellulose, and pyranoid ring skeletal vibrations of C–O–C respectively. The band at 897 cm^{-1} corresponds to the b-glycosidic linkages. FT-IR spectrum of ionic liquid anchored cellulose (Cell/IL) was shown the bond at 1648 and 1427 cm^{-1} can be assigned to the C=N and C=C due to stretching vibrations in the imidazolium rings, respectively (Shojaei et al. 2017b, a). After the adsorption of Ag-AgCl NPs, a slight decrease in peaks intensity corresponding to the O-H, C-O, C-H, and C-N groups is observed that indicate binding interaction of Ag-AgCl NPs with functional groups on support. Also, the band at 3344 cm^{-1} was transferred to 3349 cm^{-1} by the adsorption of Ag-AgCl NPs.

The crystalline structure of the polyelectrolyte (Cell/IL/Ag-AgCl NPs) was inspected by an XRD pattern. As seen in Fig. 2(b), a comparison of Ag-AgCl NPs (dark line) with Cell/IL (red line), shows new peaks (2θ) at 38.27 (226), 44.45 (200), 77.39 (201) which assigned to the cubic Ag (JCPDS file: 65-2871). Also peaks at 27.97(111), 32.40(200), 46.39(220), 55.00(311), 57.64(222), 64.66(400) related to the cubic AgCl (JCPDS file: 31-1238). The particle size of the Ag-AgCl nanoparticles was estimated by the Scherrer formula to be 8 nm at 2θ = 38.27 for Ag and 15 nm at 2θ = 32.40 for Ag-AgCl.

The information of BET surface area, pore size, and pore volume of the Cell/IL and Cell/IL/Ag-AgCl NPs were also investigated by nitrogen adsorption-desorption isotherms Fig. 2(c). The pore volume and BET surface area of Cell/IL were determined as 5.92 $m^2\ g^{-1}$ and 0.025 cm^3g^{-1}, whereas after introducing Ag-AgCl nanoparticles, Cell/IL/Ag-AgCl NPs, it was reduced to 4.22 $m^2\ g^{-1}$ and 0.016 cm^3g^{-1} respectively(Table 1). Additionally, the accommodating of the Ag-AgCl nanoparticles might lead to reducing in pore volume and surface area for the Cell/IL/Ag-AgCl NPs.

Table 1. BET surface area and porosity data of the Cell/IL and Cell/IL/Ag-AgCl NPs.

Salmple	BET surface area (m^2g^{-1})	BJH Analysis	
		Pore Volume (cm^3g^{-1})	Pore diameter (nm)
Cell/IL	5.92	0.025	1.64
Cell/IL/Ag-AgCl NPs	4.22	0.016	1.85

Thermogravimetric analysis (TGA) in an N_2 atmosphere of Cell/IL/Ag-AgCl NPs sample is represented in Fig. 2(d). Curve analysis showed that two weight loss steps were beheld for composite. The first, around 50-120 °C, is related to the deprivation of adsorbed water and solvent with ~6% weight loss. The next step around 250–450 °C with ~41.8% weight loss is attributed to the breakdown of the organic and inorganic moieties (cellulosic, ionic liquid parts and, Ag-AgCl NPs) (Shojaei et al. 2017b). Additionally, no

residue was observed after burning cellulose, while the Cell/IL/Ag-AgCl NPs had weight residue, which indicated the existence of silver in the macromolecule. Meanwhile, due to the presence of silver nanoparticles, Cell/IL/Ag-AgCl NPs had higher residuals which showed that the thermal stability of the cellulose after adding Ag nanoparticles was ameliorated.

In the process of Ag-AgCl NPs synthesis, cellulose acted as a successfully protecting support to resist the agglomeration Ag-AgCl NPs and also as a reducing agent for Ag^+ to metallic silver. The microstructures of synthesized composites were analyzed by SEM and TEM studies (Fig. 3). For Cell/IL/Ag-AgCl NPs composite, dark Ag nanoparticles were anchored on cellulose and a light black AgCl layer surrounded the around of Ag NPs (Fig. 3d). The TEM analysis confirmed that the Ag-AgCl NPs are spherical in shape and also revealed that the particles are well separated, not aggregated with an average particles size at approximately ~3 nm (Fig. 3e).

To identify elements in the Cell/IL/Ag-AgCl NPs, EDX analysis was also conducted (Fig. 3f). The presence of C, O, N, Ag, and Cl elements in the nanocomposite indicates the incorporation of silver into the polyelectrolyte surface.

The Ag nanoparticles distribution on the polyelectrolyte was appraised by EDX mapping. As shown in Fig. 4, the homogeneous density of Ag nanoparticles has been diffused on the surface of the cellulosic sample. It can be determined that the combining XRD analysis with these supportive results, indicated the successful synthesis of Ag-AgCl NPs.

Antibacterial activity of Cell/IL/Ag-AgCl NPs

In this research, the in-vitro antibacterial activity of Cell/IL/Ag-AgCl NPs was evaluated against methicillin-resistant *staphylococcus aureus* (ATCC 43300) and multidrug-resistant *Pseudomonas aeruginosa* (ATCC 27853). The antibacterial effect (MICs and MBCs values) of the compound against the bacteria evaluated was demonstrated in Fig. 5.

Our studies displayed that the antimicrobial effect of Cell/IL/Ag-AgCl NPs against *Pseudomonas aeruginosa* was higher than that of *Staphylococcus aureus.* Previous studies have shown that cellulose nanocomposites are able to inhibit the growth of infectious agents(Morones et al. 2005; Yan et al. 2016). Numerous reports on cellulosic substances and similar compounds confirm our findings(Konwarh et al. 2013; da Silva Dannenberg et al. 2017; Burdușel et al. 2018). It seems that Cell/IL/Ag-AgCl NPs (due to their biocompatible nature, good toughness, relatively low cost, and large surface area) could be used as a substitute for common antibiotics in the future, killing multidrug-resistant bacteria(Kalwar and Shen 2019b). On the other hand, using the microtiter plate method, the antibiofilm effect of this compound against bacteria was shown. This effect against *Pseudomonas aeruginosa* was remarkable (Fig. 6). It is possible that the use of these compounds can inhibit the biofilm formation of bacteria on surfaces and equipment, which in turn can reduce nosocomial infections, especially in the intensive care unit, surgery unit/room in the hospital(Marambio-Jones and Hoek 2010; Hasanzadeh et al. 2021).

Toxicity of the Cell/IL/Ag-AgCl NPs

To assess the toxic effects of the Cell/IL/Ag-AgCl NPs, human intestinal Caco-2 cells were acted with multifold concentrations of the synthesized material (0, 100, 200, 300, 400 ppm) for 24h. According to our results Fig. 7, different doses of Cell/IL/Ag-AgCl NPs up to 400 ppm did not show a significant decrease in the on cell viability compared with the control. These results are in line with previous studies that low concentrations of silver nanoparticles are nontoxic(Nguyen et al. 2017).

Our results also showed that cellulosic materials with excellent physical and biological properties are favorable candidates for biomedical products due to their low cytotoxicity, biodegradability, and biocompatibility(Annamalai and Nallamuthu 2016).

Conclusions

To enhance the efficiency of medical applications of Ag nanoparticles, a stepwise synthesis of polyelectrolyte cellulose-based macromolecule was successfully synthesized and applied in the generation and immobilization of Ag-AgCl NPs. An ionic liquid anchored Cellulose(Cell/IL) was planned to elevate the capacity for Ag nanoparticles. In the next step, Ag-AgCl was generated and loaded on modified support. In this process, renewable cellulose acts as a reducer and stabilizer of silver nanoparticles

The in vitro antibacterial activity showed that the synthesized composite has a high antimicrobial effect against *Pseudomonas aeruginosa* and *Staphylococcus aureus*. Also, the antibiofilm property of this composite against *Pseudomonas aeruginosa* was remarkable. Furthermore, the cytotoxicity study revealed low toxic effects for Ag-AgCl nanoparticles and Cell/IL support which were further confirmed in biomedical products.

Declarations

Acknowledgment

The authors would like to acknowledge the financial support of Maragheh University of Medical Sciences (grant number: n1.64.2881 and Ethical Code: IR.MARAGHEHPHC.REC.1398.030)

Declaration of Competing Interest

The authors declare no competing financial interests.

Authors Information

S. Shojaei: Email: salman.shojaei@gmail.com, ORCID: 0000-0001-8759-5331;

B. Gholipour: Email: b.gholipour@ut.ac.ir, ORCID: 0000-0002-0542-0659;

S. Rostamnia: ORCID: 0000-0001-6310-8754; Organic and Nano Group (ONG), Department of Chemistry, Iran University of Science and Technology (IUST), Tehran, Iran. Email: rostamnia@iust.ac.ir, srostamnia@gmail.com;

A. Hasanzade: Maragheh University of Medical Sciences, Maragheh, Iran.
Email: amir.hasanzadeh61@yahoo.com, ORCID: 0000-0003-2893-4369

References

1. Annamalai J, Nallamuthu T (2016) Green synthesis of silver nanoparticles: characterization and determination of antibacterial potency. Appl Nanosci 6:259–265. https://doi.org/10.1007/s13204-015-0426-6
2. Azis T, Nurdin M, Riadi LS, Arham Z, Irwan I, Salim L, Maulidiyah M (2021) Photoelectrocatalytic performance of ilmenite($FeTiO_3$) doped TiO_2/Ti electrode for reactive green 19 degradation in the UV-visible region. J Phys Conf Ser 1899. https://doi.org/10.1088/1742-6596/1899/1/012041
3. Burdușel A-C, Gherasim O, Grumezescu AM, Mogoantă L, Ficai A, Andronescu A (2018) Biomedical applications of silver nanoparticles: an up-to-date overview. Nanomaterials 8:681. https://doi.org/10.3390/nano8090681
4. Carvalho SM, Leonel AG, Mansur AAP, Carvalho C, Krambrock K, Mansur S (2019) Bifunctional magnetopolymersomes of iron oxide nanoparticles and carboxymethylcellulose conjugated with doxorubicin for hyperthermo-chemotherapy of brain cancer cells. Biomater Sci 7:2102–2122. https://doi.org/10.1039/c8bm01528g
5. da Silva Dannenberg G, Funck GD, dos Santos Cruxen CE (2017) Essential oil from pink pepper as an antimicrobial component in cellulose acetate film: Potential for application as active packaging for sliced cheese. LWT-Food Sci Technol 81:314–318. https://doi.org/ 10.1016/j.lwt.2017.04.002
6. Devi TB, Ahmaruzzaman M (2016) Bio-inspired sustainable and green synthesis of plasmonic Ag/AgCl nanoparticles for enhanced degradation of organic compound from aqueous phase. Environ Sci Pollut Res 23:17702–17714. https://doi.org/10.1007/s11356-016-6945-1
7. Dong YY, Zhu YH, Ma MG (2021) Synthesis and characterization of Ag@AgCl-reinforced cellulose composites with enhanced antibacterial and photocatalytic degradation properties. Sci Rep 11. https://doi.org/10.1038/s41598-021-82447-2
8. Ebrahimi A, Jafari N, Ebrahimpour K (2021) A novel ternary heterogeneous TiO2/BiVO4/NaY-Zeolite nanocomposite for photocatalytic degradation of microcystin-leucine arginine (MC-LR) under visible light. Ecotoxicol Environ Saf 210:111862. https://doi.org/10.1016/j.ecoenv.2020.111862
9. Ghasemi Z, Shojaei S, Shahrisa A (2016) Copper iodide nanoparticles supported on magnetic aminomethylpyridine functionalized cellulose: a new heterogeneous and recyclable nanomagnetic catalyst for facile access to N-sulfonylamidines under solvent free conditions. RSC Adv 6:56213–56224. https://doi.org/10.1039/C6RA13251K

10. Guan X, Lin S, Lan J (2019) Fabrication of Ag/AgCl/ZIF-8/TiO2 decorated cotton fabric as a highly efficient photocatalyst for degradation of organic dyes under visible light. Cellulose 26:7437–7450. https://doi.org/10.1007/s10570-019-02621-8
11. Han C, Ge L, Chen C (2014) Site-selected synthesis of novel Ag@AgCl nanoframes with efficient visible light induced photocatalytic activity. J Mater Chem A 2:12594–12600. https://doi.org/10.1039/c4ta01941e
12. Hasanzadeh A, Gholipour B, Rostamnia S (2021) Biosynthesis of AgNPs onto the urea-based periodic mesoporous organosilica (AgxNPs/Ur-PMO) for antibacterial and cell viability assay. J Colloid Interface Sci 585:676–683. https://doi.org/10.1016/j.jcis.2020.10.047
13. Hayati P, Mehrabadi Z, Karimi M (2021) Photocatalytic activity of new nanostructures of an Ag(i) metal-organic framework (Ag-MOF) for the efficient degradation of MCPA and 2,4-D herbicides under sunlight irradiation. New J Chem 45:3408–3417. https://doi.org/10.1039/d0nj02460k
14. Heidarpour H, Golizadeh M, Padervand M (2020) In-situ formation and entrapment of Ag/AgCl photocatalyst inside cross-linked carboxymethyl cellulose beads: A novel photoactive hydrogel for visible-light-induced photocatalysis. J Photochem Photobiol A Chem. https://doi.org/10.1016/j.jphotochem.2020.112559. 398:
15. Jin T, He Y (2011) Antibacterial activities of magnesium oxide (MgO) nanoparticles against foodborne pathogens. J Nanoparticle Res 13:6877–6885. https://doi.org/10.1007/s11051-011-0595-5
16. Kalwar K, Shen M (2019a) Electrospun cellulose acetate nanofibers and Au@AgNPs for antimicrobial activity-A mini review. Nanotechnol Rev 8:246–257. https://doi.org/10.1515/ntrev-2019-0023
17. Klemm D, Kramer F, Moritz S (2011) Nanocelluloses: a new family of nature-based materials. Angew Chemie Int Ed 50:5438–5466. https://doi.org/10.1002/anie.201001273
18. Ko JW, Lee B, Il, Chung YJ, Park CB (2015) hierarchically structured metal oxides †. https://doi.org/10.1039/c5gc01348h
19. Konwarh R, Karak N, Misra M (2013) Electrospun cellulose acetate nanofibers: the present status and gamut of biotechnological applications. Biotechnol Adv 31:421–437. https://doi.org/10.1016/j.biotechadv.2013.01.002
20. León-Silva S, Fernández-Luqueño F, López-Valdez F (2016) Silver Nanoparticles (AgNP) in the Environment: a Review of Potential Risks on Human and Environmental Health. Water Air Soil Pollut. .. org/10.1007/s11270-016-3022-9. https://doi.org/10.1007/s11270-016-3022-9227:
21. Leonel AG, Mansur HS, Mansur AAP (2019) Synthesis and characterization of iron oxide nanoparticles/carboxymethyl cellulose core-shell nanohybrids for killing cancer cells in vitro. Int J Biol Macromol 132:677–691. https://doi.org/10.1016/j.ijbiomac.2019.04.006
22. Lv J, Zhang X, Yu N (2019) One-pot synthesis of CNC-Ag@AgCl with antifouling and antibacterial properties. Cellulose 26:7837–7846. https://doi.org/10.1007/s10570-019-02658-9
23. Marambio-Jones C, Hoek EMV (2010) A review of the antibacterial effects of silver nanomaterials and potential implications for human health and the environment. J nanoparticle Res 12:1531–

1551. https://doi.org/ 10.1007/s11051-010-9900-y

24. Mohammed N, Grishkewich N, Tam KC (2018) Cellulose nanomaterials: promising sustainable nanomaterials for application in water/wastewater treatment processes. Environ Sci Nano 5:623–658. https://doi.org/10.1039/C7EN01029J
25. Moon RJ, Martini A, Nairn J et al (2011) Cellulose nanomaterials review: structure, properties and nanocomposites. Chem Soc Rev 40:3941–3994. https://doi.org/ 10.1039/C0CS00108B
26. Morones JR, Elechiguerra JL, Camacho A (2005) The bactericidal effect of silver nanoparticles. Nanotechnology 16:2346. https://doi.org/ 10.1088/0957–4484/16/10/059
27. Nguyen THD, Vardhanabhuti B, Lin M, Mustapha A (2017) Antibacterial properties of selenium nanoparticles and their toxicity to Caco-2 cells. Food Control 77:17–24. https://doi.org/ 10.1016/j.foodcont.2017.01.018
28. Pasquet J, Chevalier Y, Couval E (2014) Antimicrobial activity of zinc oxide particles on five micro-organisms of the Challenge Tests related to their physicochemical properties. Int J Pharm 460:92–100. https://doi.org/10.1016/j.ijpharm.2013.10.031
29. Patil MP, Palma J, Simeon NC (2017) Sasa borealis leaf extract-mediated green synthesis of silver-silver chloride nanoparticles and their antibacterial and anticancer activities. New J Chem 41:1363–1371. https://doi.org/10.1039/c6nj03454c
30. Pinkert A, Marsh KN, Pang S, Staiger MP (2009) Ionic liquids and their interaction with cellulose. Chem Rev 109:6712–6728. https://doi.org/ 10.1021/cr9001947
31. Qi X, Chen H, Rui Y (2015) Floating tablets for controlled release of ofloxacin via compression coating of hydroxypropyl cellulose combined with effervescent agent. Int J Pharm 489:210–217. https://doi.org/1 0.1016/j.ijpharm.2015.05.007
32. Qin J, Wang Z, Hu J et al (2022) Distinct liquid crystal self-assembly behavior of cellulose nanocrystals functionalized with ionic liquids. Colloids Surf Physicochem Eng Asp 632:127790. https://doi.org/10.1016/j.colsurfa.2021.127790
33. Rahimi M, Shojaei S, Safa KD et al (2017) Biocompatible magnetic tris (2-aminoethyl) amine functionalized nanocrystalline cellulose as a novel nanocarrier for anticancer drug delivery of methotrexate. New J Chem 41:2160–2168. https://doi.org/ 10.1039/C6NJ03332F
34. Riduan SN, Yuan Y, Zhou F et al (2016) Ultrafast killing and self-gelling antimicrobial imidazolium oligomers. Small 12:1928–1934. https://doi.org/10.1002/smll.201600006
35. Rostamnia S, Doustkhah E, Estakhri S, Karimi Z (2016) Layer by layer growth of silver chloride nanoparticle within the pore channels of SBA-15/SO3H mesoporous silica (AgClNP/SBA-15/SO3K): Synthesis, characterization and antibacterial properties. Phys E Low-Dimensional Syst Nanostructures 76:146–150. https://doi.org/10.1016/j.physe.2015.10.026
36. Ruparelia JP, Chatterjee AK, Duttagupta SP, Mukherji S (2008) Strain specificity in antimicrobial activity of silver and copper nanoparticles. Acta Biomater 4:707–716. https://doi.org/10.1016/j.actbio.2007.11.006

37. Sattari R, Khayati GR, Hoshyar R (2021) Biosynthesis of Silver–Silver Chloride Nanoparticles Using Fruit Extract of Levisticum Officinale: Characterization and Anticancer Activity Against MDA-MB-468 Cell Lines. J Clust Sci 32:593–599. https://doi.org/10.1007/s10876-020-01818-3
38. Shafiei-Irannejad V, Rahimi M, Zarei M (2019) Polyelectrolyte carboxymethyl cellulose for enhanced delivery of doxorubicin in MCF7 breast cancer cells: toxicological evaluations in mice model. Pharm Res 36:1–17. https://doi.org/10.1007/s11095-019-2598-3
39. Shojaei S, Ghasemi Z, Shahrisa A (2017a) Three-component synthesis of N-sulfonylformamidines in the presence of magnetic cellulose supported N-heterocyclic carbene-copper complex, as an efficient heterogeneous nanocatalyst. Tetrahedron Lett 58:3957–3965. https://doi.org/10.1016/j.tetlet.2017.08.075
40. Shojaei S, Ghasemi Z, Shahrisa A (2017b) Cu (I)@ Fe3O4 nanoparticles supported on imidazolium-based ionic liquid-grafted cellulose: Green and efficient nanocatalyst for multicomponent synthesis of N-sulfonylamidines and N-sulfonylacrylamidines. Appl Organomet Chem 31:e3788. https://doi.org/10.1002/aoc.3788
41. Smiechowicz E, Niekraszewicz B, Kulpinski P, Dzitko K (2018) Antibacterial composite cellulose fibers modified with silver nanoparticles and nanosilica. Cellulose 25:3499–3517. https://doi.org/10.1007/s10570-018-1796-1
42. Van Den Hurk J, Havel V, Linn E (2013) Ag/GeSx /Pt-based complementary resistive switches for hybrid CMOS/Nanoelectronic logic and memory architectures. Sci Rep 3:2–6. https://doi.org/10.1038/srep02856
43. Vargas-Reus MA, Memarzadeh K, Huang J (2012) Antimicrobial activity of nanoparticulate metal oxides against peri-implantitis pathogens. Int J Antimicrob Agents 40:135–139. https://doi.org/10.1016/j.ijantimicag.2012.04.012
44. Vilamová Z, Konvičková Z, Mikeš P (2019) Ag-AgCl Nanoparticles Fixation on Electrospun PVA Fibres: Technological Concept and Progress. Sci Rep 9:1–10. https://doi.org/10.1038/s41598-019-51642-7
45. Wang G, Li F, Li L (2020) In Situ Synthesis of Ag-Fe3O4 Nanoparticles Immobilized on Pure Cellulose Microspheres as Recyclable and Biodegradable Catalysts. ACS Omega 5:8839–8846. https://doi.org/10.1021/acsomega.0c00437
46. Wang L, Clavero C, Huba Z (2011) Plasmonics and enhanced magneto-optics in core-shell Co-Ag nanoparticles. Nano Lett 11:1237–1240. https://doi.org/10.1021/nl1042243
47. Wu Y, Chen S, Guo X (2017) Environmentally benign chitosan as precursor and reductant for synthesis of Ag/AgCl/N-doped carbon composite photocatalysts and their photocatalytic degradation performance. Res Chem Intermed 43:3677–3690. https://doi.org/10.1007/s11164-016-2835-x
48. Yan J, Abdelgawad AM, El-Naggar ME, Rojas OJ (2016) Antibacterial activity of silver nanoparticles synthesized In-situ by solution spraying onto cellulose. Carbohydr Polym 147:500–508. https://doi.org/10.1016/j.carbpol.2016.03.029

49. Yuan Y, Ding L, Chen Y (2021) Nano-silver functionalized polysaccharides as a platform for wound dressings: A review. Int J Biol Macromol. https://doi.org/10.1016/j.ijbiomac.2021.11.108

Schemes

Schemes 1 is available in the Supplementary Files section

Figures

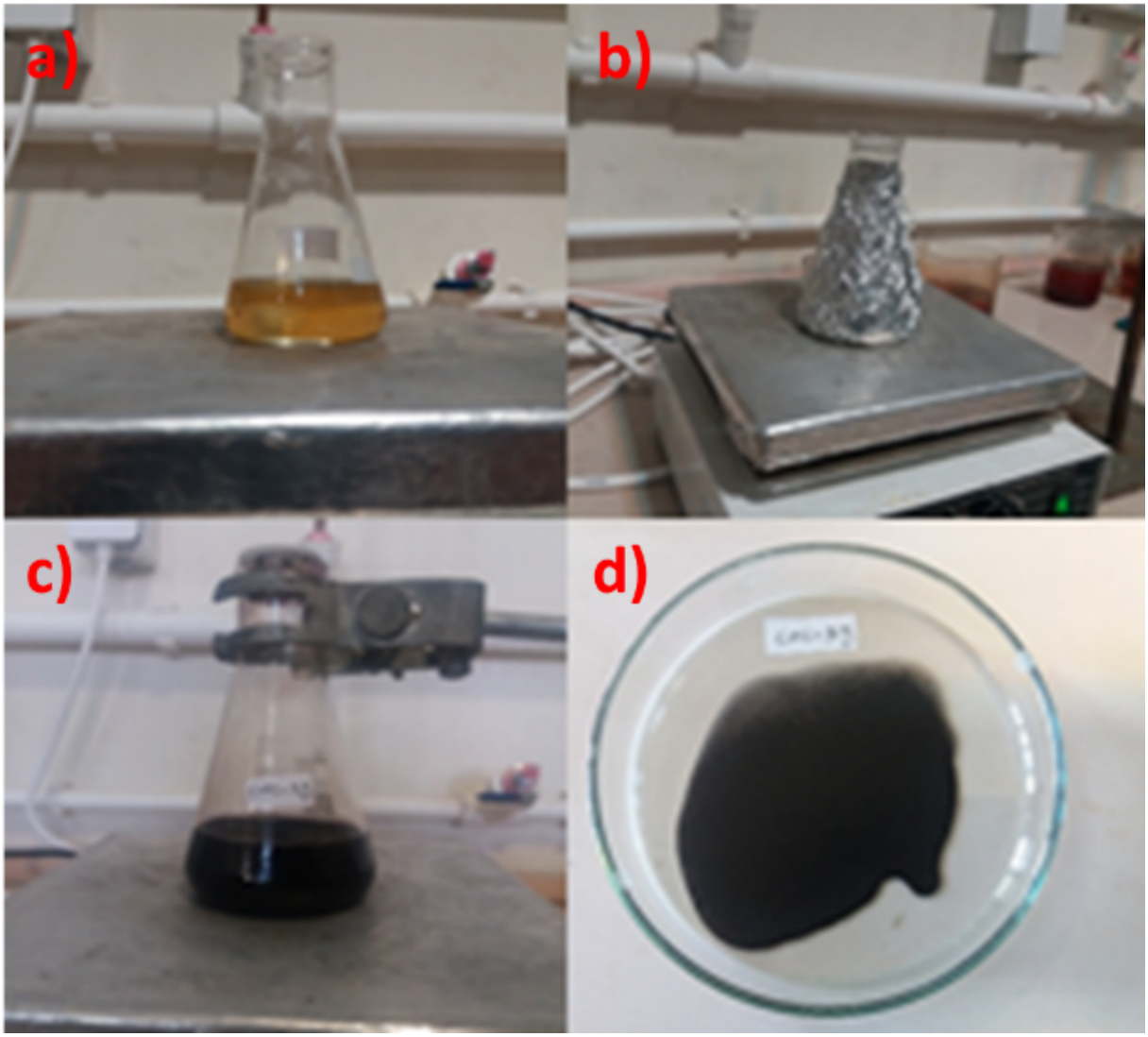

Figure 1

Preparation of Ag-AgCl nanoparticles supported on ionic liquid anchored cellulose.

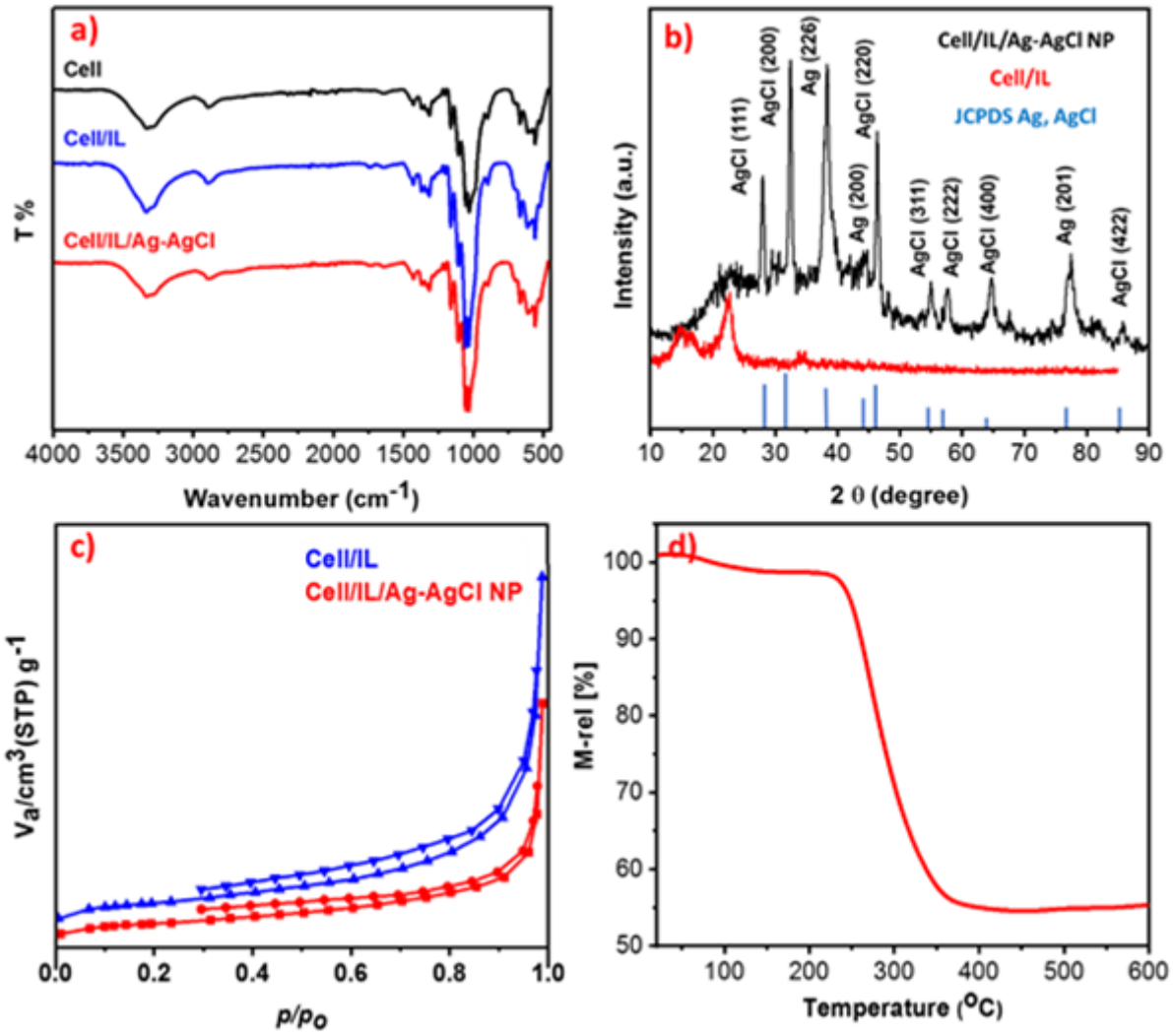

Figure 2

(a) FT-IR spectra, (b) XRD pattern, (c) Nitrogen adsorption-desorption isotherms of Cell/IL and Cell/IL/Ag-AgCl NPs, and (d) TGA thermogram of Cell/IL/Ag-AgCl NPs in N2 atmosphere.

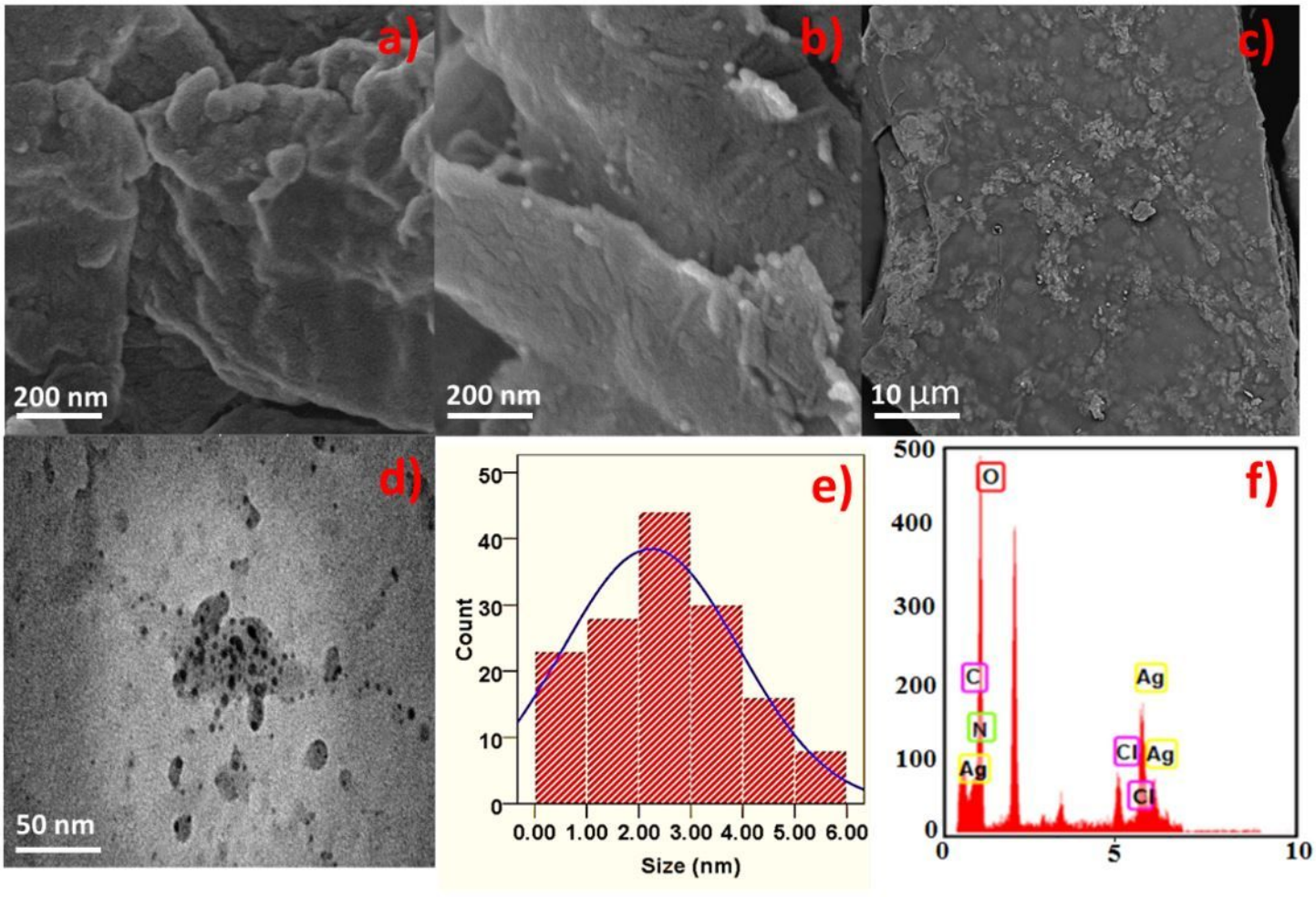

Figure 3

SEM images of Cellulose (a), Cell/IL (b), Cell/IL/Ag-AgCl NPs (c); TEM image of Cell/IL/Ag-AgCl NPs (d); particle size distribution of Ag-AgCl NPs (e) and EDX analysis diagrams of Cell/IL/Ag-AgCl NPs (f).

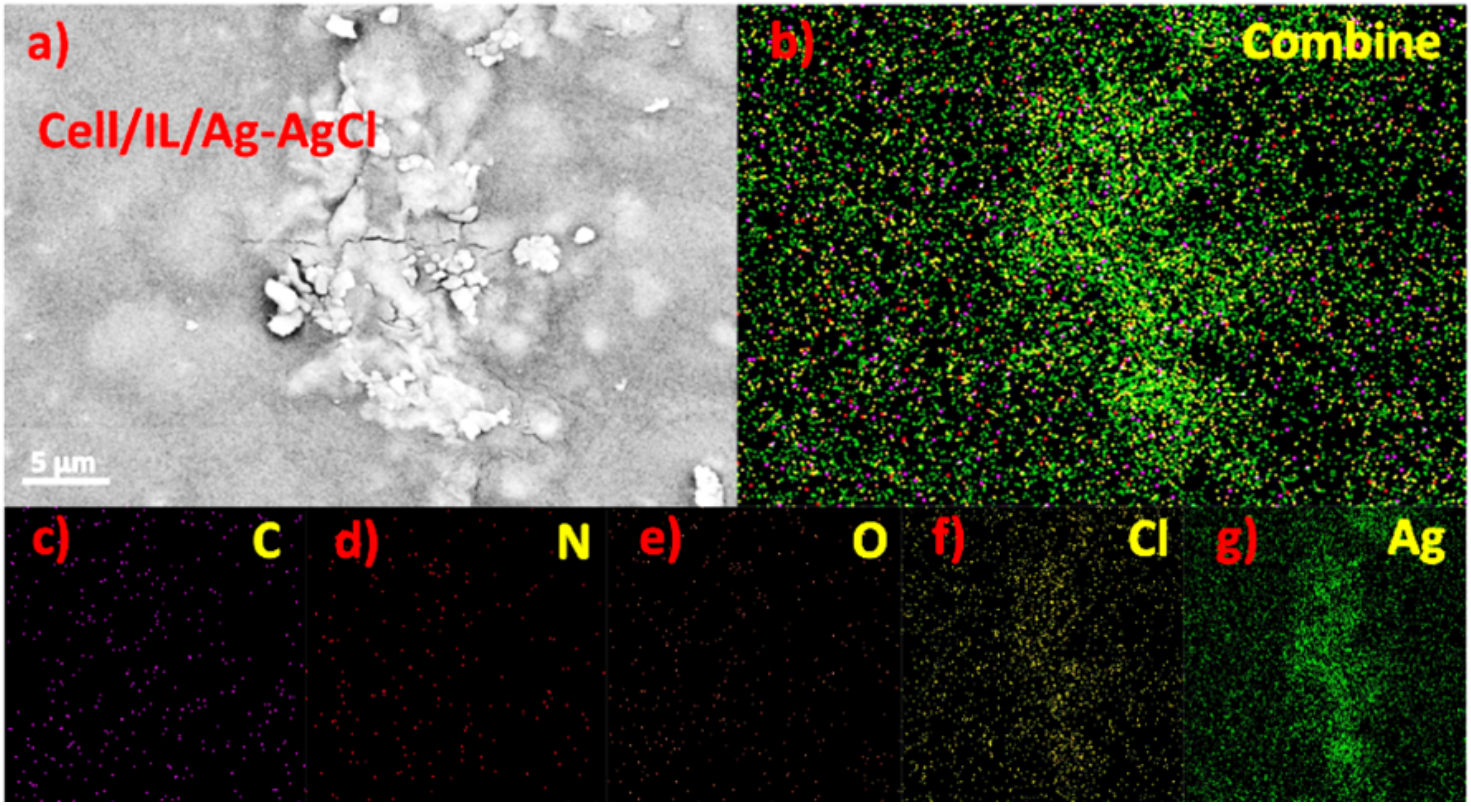

Figure 4

(a) SEM image and (b) EDX elemental mapping of Cell/IL/Ag-AgCl NPs; (c) carbon, (d) nitrogen, (e) oxygen, (f) chlorine and (g) silver.

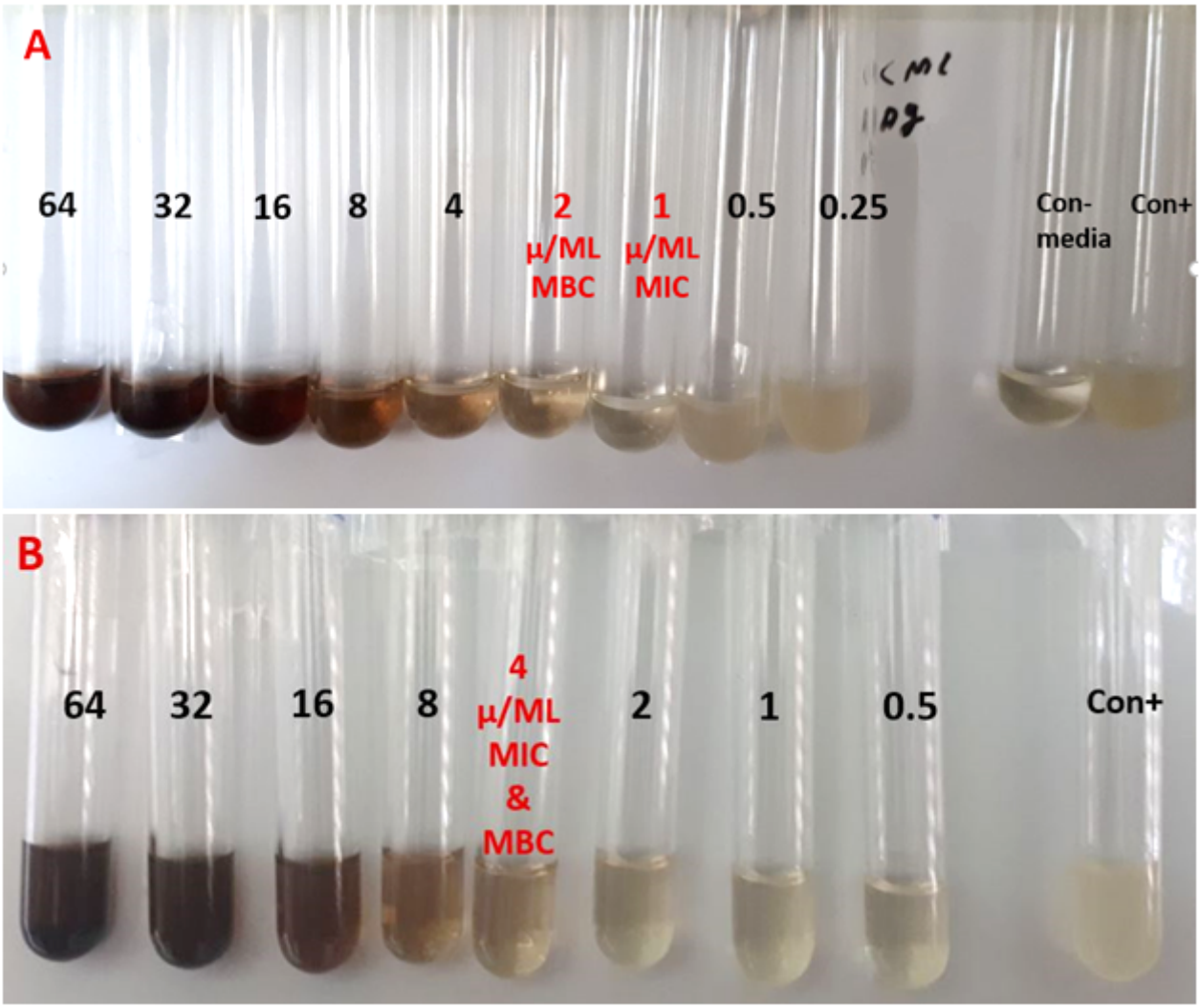

Figure 5

MICs[a] and MBCs[b] values of the synthesized compound against Pseudomonas aeruginosa ATCC 27853 (A) and Staphylococcus aureus ATCC 43300 (B).

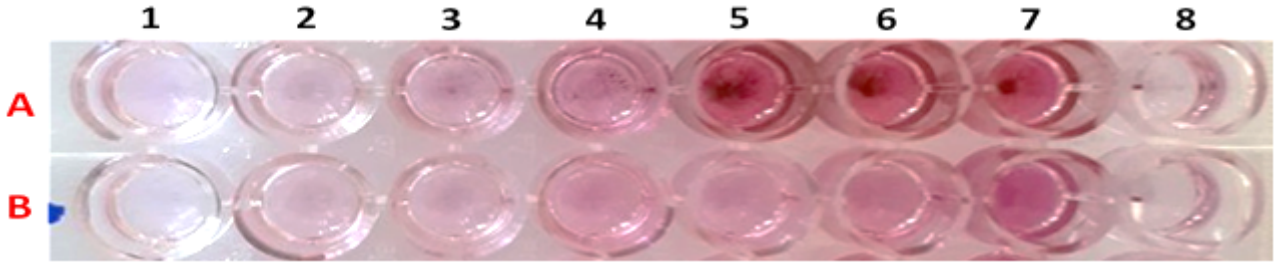

Figure 6

Antibiofilm activity of Cell/IL/Ag-AgCl NPs against *Staphylococcus aureus* ATCC 15442 (A) and *Pseudomonas aeruginosa* ATCC 35556 (B). Cell/IL/Ag-AgClNPs concentrations in wells 1 through 6 are:

32, 16, 8, 4, 2 and 1 µg/ml. Wells 7 and 8 are positive and negative controls, respectively.

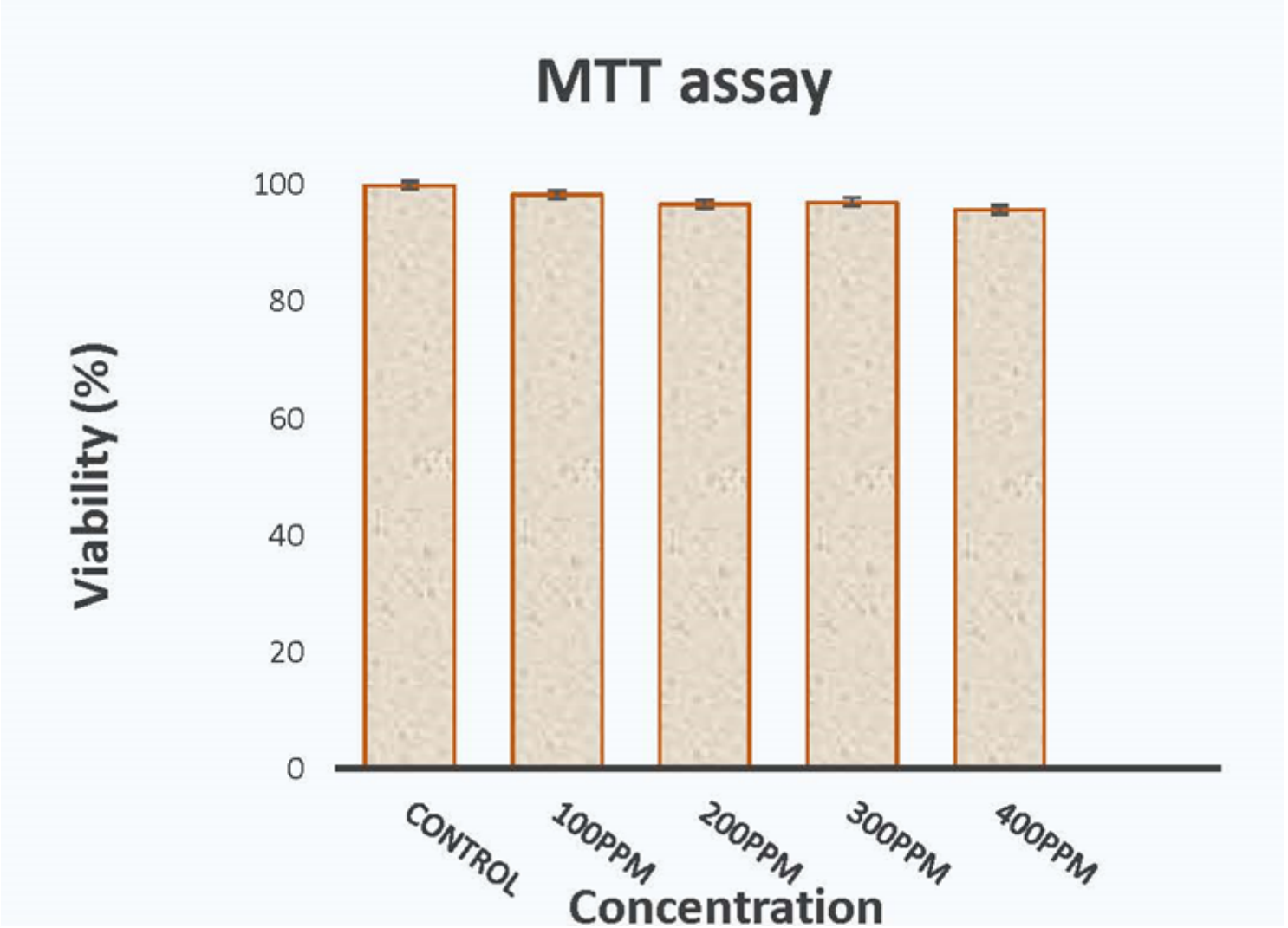

Figure 7

Cell death induction by Cell/IL/Ag-AgCl NPs in Caco-2 cells. Cells were exposed to different concentrations of Cell/IL/Ag-AgCl NPs (0, 100, 200, 300, 400 ppm) for 24 h cell toxicity was measured by MTT test. Data represent the mean ± S.E.M. (n=6).

Supplementary Files

This is a list of supplementary files associated with this preprint. Click to download.

- Scheme1.jpg